

Quantum critical behavior in strongly interacting Rydberg gases

Hendrik Weimer,¹ Robert Löw,² Tilman Pfau,² and Hans Peter Büchler¹

¹*Institute of Theoretical Physics III, Universität Stuttgart, 70550 Stuttgart, Germany**

²*5. Physikalisches Institut, Universität Stuttgart, 70550 Stuttgart, Germany*

(Dated: October 26, 2018)

We study the appearance of correlated many-body phenomena in an ensemble of atoms driven resonantly into a strongly interacting Rydberg state. The ground state of the Hamiltonian describing the driven system exhibits a second order quantum phase transition. We derive the critical theory for the quantum phase transition and show that it describes the properties of the driven Rydberg system in the saturated regime. We find that the suppression of Rydberg excitations known as blockade phenomena exhibits an algebraic scaling law with a universal exponent.

PACS numbers: 05.70.Jk, 32.80.Ee, 02.70.-c, 42.50.Ct

The concept of universality is a powerful tool for the understanding and characterization of complex phenomena in different fields of physics. The most pronounced example represents the universal scaling in systems close to a second order phase transition and the characterization of the transition in terms of critical theories and universality classes [1]. Its main assertion is that in the presence of a diverging length scale, physical observables become independent on the precise microscopic realization of the systems, and allows for a qualitative understanding without the knowledge of the exact microscopic details. In this Letter, we analyze the appearance of correlated manybody effects in a dense ensemble of atoms driven resonantly in a strongly interacting Rydberg state, and show that the behavior of the system can be understood in terms of a critical theory.

Strongly interacting Rydberg atoms are an area of intense experimental investigation: the resonant diffusion of Rydberg excitations via the dipole-dipole interactions has been reported [2], and the reduction of Rydberg excitation due to blockade effects has been observed [3, 4, 5, 6, 7, 8]. Furthermore, coherent optical excitation has been observed for individual Rydberg atoms [9], essentially non-interacting ensembles [10, 11, 12], as well as in the strongly interacting regime [7]. Of special interest for the theoretical analysis are cold atomic samples, where the thermal motion of the atoms is essentially frozen on the characteristic time scale of the Rydberg excitation (“frozen Rydberg gas”) [2]. Then, the time evolution of such an atomic ensemble driven by a resonant Rydberg excitation has been extensively studied in the past using a numerical integration of the time-dependent Schrödinger equation for small sample sizes [13, 14] and within a master equation approach [15, 16].

In contrast to the previous analyses studying the time evolution, the approach for the study of strongly interacting Rydberg gases presented in this Letter is based on the observation that the driven system relaxes into an equilibrium state. This equilibrium state is dominated by the thermodynamic phases of the Hamiltonian describing the driven system, which exhibits a continuous quantum

phase transition in the detuning Δ ; see Fig. 1(a). Then, the resonant regime with $\Delta = 0$ is determined by the critical properties of the phase transition. We derive the universal exponents within mean-field theory, and show that the time evolution of the system and its relaxation into the equilibrium state is well described by a master equation derived from the microscopic Hamiltonian.

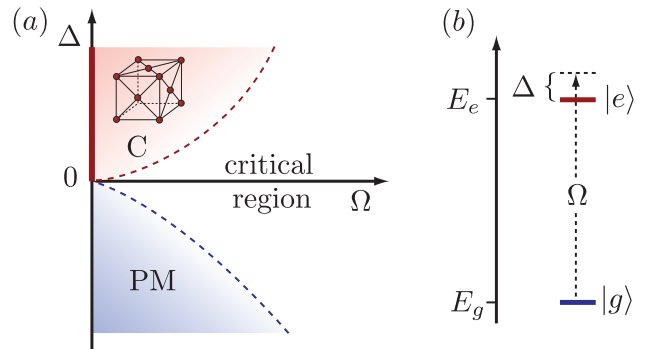


FIG. 1: (color online). (a) Phase diagram in the Δ - Ω -plane: for a coupling $\Omega = 0$ a second order phase transition appears from a crystalline phase (C) to a paramagnetic phase (PM), while at a detuning $\Delta = 0$ the system is dominated by the critical region. (b) Setup of the system with $|g\rangle$ the atomic ground state and $|e\rangle$ the excited Rydberg state coupled by driving lasers with Rabi frequency Ω and detuning Δ .

We start with the Hamiltonian describing an ultracold gas of atoms driven into an excited Rydberg state with a repulsive van der Waals interaction. The relevant internal structure for each atom is given by the atomic ground state $|g\rangle_i$ and the excited Rydberg state $|e\rangle_i$, reducing the internal structure to a two-level system. The two internal states are coherently coupled by external lasers with the Rabi frequency Ω and a detuning Δ ; see Fig. 1(b). The characteristic time scale for a Rydberg excitation is short compared to the thermal motion of each atom, and the positions \mathbf{r}_i of the atoms are frozen [2]: the positions \mathbf{r}_i are randomly distributed according to the distribution function of a thermal gas. After performing the rotating wave approximation, the Hamiltonian in the rotating

frame can be written as a spin Hamiltonian (cf. [13])

$$\hat{H} = -\frac{\Delta}{2} \sum_i \hat{\sigma}_z^{(i)} + \frac{\hbar\Omega}{2} \sum_i \hat{\sigma}_x^{(i)} + C_6 \sum_{j<i} \frac{\hat{P}_{ee}^{(i)} \hat{P}_{ee}^{(j)}}{|\mathbf{r}_i - \mathbf{r}_j|^6}, \quad (1)$$

where $\hat{P}_{ee}^{(i)} = |e\rangle_i \langle e|_i = (1 + \hat{\sigma}_z^{(i)})/2$ is the projector onto the excited Rydberg state of the i^{th} atom. The last term accounts for the strong van der Waals repulsion between the Rydberg states with $C_6 \propto \bar{n}^{11}$, where \bar{n} is the principle quantum number of the Rydberg excitation [17, 18]. It is well known that dense samples of Rydberg atoms undergo collective ionization processes that might harm the coherent evolution [19]. However for repulsive Rydberg S states these ionization processes are slowed down significantly [20]. Recent experiments in very dense samples allowed to follow the coherent evolution involving Rydberg S states on timescales comparable to the timescales required to reach equilibrium [6, 7]. In these experiments the saturation is reached well before radiative or motional decoherence effects set in. Therefore the validity of the Hamiltonian (1) is well justified for an experimentally realistic situation.

Within the standard experimental setup, the system is prepared with all the atoms in the ground state and the time evolution is studied by turning on the excitation lasers, i.e., $|\psi\rangle = \prod_i |g\rangle_i$. While in absence of interactions, the time evolution of the Hamiltonian (1) results in coherent Rabi oscillations for each atom with the reduced density matrix for each atom being a pure state, the interactions leads to correlations between different atoms, and eventually to a decoherence of this single atom pure state. Consequently, the density matrix describing a subsystem of the atomic cloud will equilibrate into a steady state under time evolution as the surrounding atomic states act as a reservoir interacting with the subsystem. This behavior is well confirmed by the exact numerical integration of the system with the Hamiltonian (1), see below, and is also observed in experiments via the saturation of the Rydberg excitation [6]. This observation opens up an alternative approach to study the long-time behavior of the system by focusing on the equilibrium states of the Hamiltonian (1), and especially on its zero temperature phase diagram.

For vanishing Rabi frequency $\Omega = 0$, the exact ground state of the Hamiltonian (1) can be analytically determined in any dimension. It is dominated by a second order quantum phase transition for the critical detuning $\Delta_c = 0$; see Fig. 1. For negative detuning $\Delta \leq 0$ the ground state is paramagnetic with all atoms in the atomic state $|g\rangle_i$; i.e., the experimentally relevant initial state $|\psi\rangle$ is the ground state of the system. In turn for positive detuning $\Delta > 0$, the ground state prefers to excite atoms into the Rydberg state and the configuration minimizing the repulsive van der Waals interaction is obtained for a crystalline arrangement of the atoms. It is important to notice, that within the critical region the

system is independent on the microscopic realization, and therefore, its properties are isotropic and homogeneous.

The behavior of the system for finite Ω in the resonant regime $\Delta = 0$ is dominated by the critical behavior of the second order quantum phase transition. At the critical point with $\Delta = 0$, the system is characterized by a single dimensionless parameter $\alpha = \hbar\Omega/C_6 n^2$ describing the ratio between the coupling energy $\hbar\Omega$ and the interaction energy $C_6 n^2$ (here, n denotes the atomic density). Then, the ground state properties such as the fraction of excited Rydberg atoms exhibit an algebraic behavior

$$f_R \equiv \langle P_{ee}^{(i)} \rangle = c\alpha^\nu, \quad (2)$$

with a universal scaling exponent ν in the critical region with $\alpha \ll 1$. In the following, we determine the critical exponent within mean-field theory.

The important quantity in the mean-field theory is the averaged Rydberg fraction $f_R = \langle P_{ee}^{(i)} \rangle$. In addition, the van der Waals interaction gives rise to blockade phenomena; i.e., once a Rydberg state is excited the excitation of an additional Rydberg atom is strongly suppressed in the surrounding area characterized by a blockade radius a_R . The correct description of this property is obtained by the pair-correlation function $g_2(\mathbf{r}_i - \mathbf{r}_j) = \langle \hat{P}_{ee}^{(i)} \hat{P}_{ee}^{(j)} \rangle / f_R^2$, where $g_2(\mathbf{r})$ vanishes in the blocked region for $|\mathbf{r}| \ll a_R$, while at large distances $|\mathbf{r}| \gg a_R$ the correlation disappears and $g_2(\mathbf{r}) = 1$. The transition from a strong suppression to the uncorrelated regime is very sharp due to the van der Waals repulsion [13], and the pair-correlation function is well described by a step function $g_2(\mathbf{r}) = \Theta(|\mathbf{r}| - a_R)$. Then, the mean-field theory is obtained by replacing the microscopic interaction by the mean interaction of the surrounding atoms

$$\hat{P}_{ee}^{(i)} \hat{P}_{ee}^{(j)} \approx \left[\hat{P}_{ee}^{(i)} f_R + \hat{P}_{ee}^{(j)} f_R - f_R^2 \right] g_2(\mathbf{r}_i - \mathbf{r}_j), \quad (3)$$

which neglects the quadratic fluctuations around the mean field and reduces the Hamiltonian to a sum of single site Hamiltonians, $\hat{H} = \sum_i \hat{H}_{\text{MF}}^{(i)}$. In the scaling regime with $\alpha \ll 1$, the number of atoms in the blocked regime is large, i.e., $a_R^3 n \gg 1$, which allows us to replace the summation over the surrounding atoms j by an integral over space with a homogeneous atomic density n . Then, we obtain the Hamiltonian for the i^{th} atom,

$$\frac{\hat{H}_{\text{MF}}^{(i)}}{E_0} = \frac{\alpha}{2} \hat{\sigma}_x^{(i)} + \frac{4\pi}{3} \frac{f_R}{na_R^3} \hat{P}_{ee}^{(i)} - \frac{2\pi}{3} \frac{f_R^2}{na_R^3} = \mathbf{h} \cdot \hat{\boldsymbol{\sigma}}^{(i)} + h_0. \quad (4)$$

with the characteristic energy scale $E_0 = C_6 n^2$. Note that in equilibrium the correlation function $g_2(\mathbf{r})$ satisfies the normalization condition $n f_R \int d\mathbf{r} [1 - g_2(\mathbf{r})] = 1$, which provides the relation $a_R = (3/4\pi f_R n)^{1/3}$. The effective Hamiltonian is equivalent to a spin in a magnetic field \mathbf{h} with $h_x = \alpha/2$ and $h_z = 8\pi^2 f_R^2/9$, and a constant energy offset $h_0 = h_z(1 - f_R)$. Using a spin rotation,

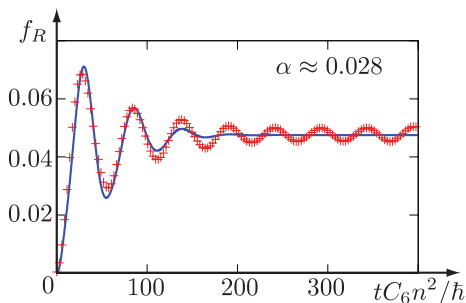


FIG. 2: (color online). Numerical integration of the full Hamiltonian (crosses) for $\alpha = 1/36$, $N = 60$ and averaged over 50 different initial conditions. The remaining oscillations at large times are finite size effects. The solution of the master equation is shown as solid line.

we can diagonalize the Hamiltonian $\hat{H}_{\text{MF}}^{(i)} = h\hat{\sigma}_{z'}^{(i)} + h_0$ with $h = \sqrt{h_x^2 + h_z^2}$. Here, $\hat{\sigma}_{z'}^{(i)} = \cos\theta\hat{\sigma}_z^{(i)} + \sin\theta\hat{\sigma}_x^{(i)}$ denotes the Pauli matrix in the new basis with the rotation angle $\tan\theta = h_x/h_z$. Within the new basis the stationary equilibrium density matrix $\hat{\rho}^{(i)}$ is diagonal. Its entries dependent on the experimental realization of the system: (i) for an adiabatic switching on of the Rabi frequency, the system remains in the ground state and the density matrix reduces to the lowest energy state of $\hat{H}_{\text{MF}}^{(i)}$. (ii) on the other hand, for a sudden switching on of the Rabi frequency, the density matrix is determined by energy conservation: the energy of the equilibrated state is equal to the energy of the initial state, i.e., $\text{Tr}\{\hat{H}_{\text{MF}}^{(i)}\hat{\rho}^{(i)}\} = \langle\psi|\hat{H}|\psi\rangle/N = 0$ (here, N denotes the total number of particles). It can be checked that the scaling exponent remains the same in both cases, indicating that the equilibrium state in the second case is close to the ground state. In the following, we focus on a sudden switching on of the Rabi frequency. The mean-field solution for the equilibrium state reduces to $\hat{\rho}^{(i)} = [1 - (h_0/h)\hat{\sigma}_{z'}^{(i)}]/2$, and a transformation into the original coordinates yields the self-consistency relation

$$f_R = \langle\hat{P}_{ee}^{(i)}\rangle = \frac{1}{2} \frac{(4\pi)^4 f_R^5 + (9\alpha)^2}{(4\pi f_R)^4 + (9\alpha)^2}. \quad (5)$$

The solution in the limit $\alpha \ll 1$ provides the critical exponent $\nu = 2/5$ with the prefactor $c = (9/16\pi^2)^{2/5}$.

The same mean-field analysis can also be performed for arbitrary dimensions $d \leq 4$. The main modification is that the dimensionless parameter $\alpha_d = \hbar\Omega/C_6 n^{6/d}$ exhibits a dependence on the dimension d and also h_z obeys the modified scaling $h_z \sim f_R^{6/d}$. The general result provides the scaling exponent $\nu_d = 2d/(12+d)$.

We now compare the above mean-field solution to numerical studies of the time evolution with the full Hamiltonian Eq. (1). We place N atoms randomly into a box of volume V having periodic boundary conditions. The dimension of the full Hilbert space grows exponentially like

2^N ; therefore, the exact dynamics can only be calculated for a relatively small number of atoms [13, 21]. However, the strong van der Waals repulsion suppresses the occupation probabilities of many basis states, which allows us to significantly reduce the Hilbert space: for each basis state we compute the van der Waals energy and remove the state if its van der Waals energy is larger than a cutoff energy E_C . This reduction leads for $N = 100$ to approximately 10^6 relevant basis states compared to the 10^{30} basis states of the full Hilbert space. Convergence has been checked by increasing E_C . We have used a fourth-order Runge-Kutta scheme for performing the numerical integration of the Schrödinger equation. The time-dependence of the Rydberg fraction $f_R(t) = \sum_i \langle P_{ee}^i \rangle / N$ is shown in Fig. 2 (crosses), for an average of 50 different uniformly distributed random initial conditions with $N = 60$ and $\alpha = 1/36$. We find a clear saturation of the excited Rydberg fraction f_R ; the remaining oscillations at large times are further suppressed for larger system sizes, and therefore represent a finite size effect.

In order to investigate the scaling behavior of the saturated Rydberg fraction f_R we have taken an average over the Rydberg fraction $f_R(t)$ for times $250 \leq tC_6 n^2 / \hbar \leq 400$ for 50 different random initial conditions. The dimensionless parameter α has been varied by changing the number of atoms from $N = 52$ to $N = 100$, and by changing C_6 from 0.01 to 0.04. The scaling behavior is shown in Fig. 3. The data show a power law dependence according to $f_R = c\alpha^\nu$. The fit to the numerical data provides an exponent $\nu = 0.404$, which is in very good agreement with the result derived in the mean-field theory. For the onedimensional case the numerically obtained critical exponent is $\nu_{1D} = 0.150$. Surprisingly, this value is again very close to the mean-field prediction, indicating that the van der Waals interaction strongly suppresses quantum fluctuations.

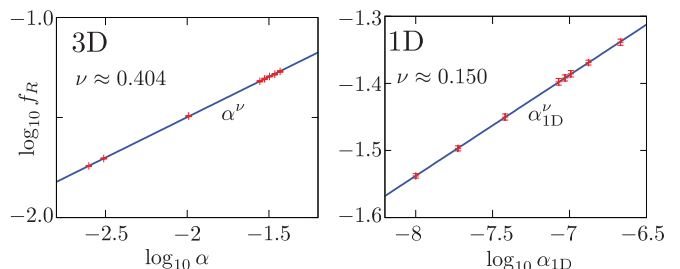


FIG. 3: (color online). Numerical results for the saturated Rydberg fraction f_R in a 3D and a 1D setup: the system exhibits an algebraic behavior $f_R \sim \alpha^\nu$ with $\nu \approx 0.404$ and $\nu_{1D} \approx 0.150$.

Finally, we are interested in a description of the time evolution and derive a master equation with the mean-field solution as its stationary state. The natural mechanisms for the equilibration into a stationary state are the residual interactions between the atoms, which go

beyond the mean-field description. We write the exact Hamiltonian (1) as a sum of the mean-field terms and the remaining fluctuations $\hat{H} = \sum_i \hat{H}_{\text{MF}}^{(i)} + \Delta\hat{H}$. The derivation of the master equation from the microscopic Hamiltonian uses the time-convolutionless projection operator method with an extended projection operator [22]: we select a single site i , which will play the role of the system with the Hamiltonian $\hat{H}_{\text{MF}}^{(i)}$, while the surrounding atoms act as the bath coupled to the system state by the Hamiltonian $\Delta\hat{H}$. The role of the pair-correlation function is to enforce the blockade regime. Here, we assume the pair-correlation function to be fixed during the time evolution. Then, its influence is well accounted for by expressing the remaining interactions as $\Delta\hat{H} = \sum_{i<j} g_2(\mathbf{r}_i - \mathbf{r}_j) C_6/|\mathbf{r}_i - \mathbf{r}_j|^6 \left(\hat{P}_{ee}^{(i)} - f_R \right) \left(\hat{P}_{ee}^{(j)} - f_R \right)$. The projection operator consistent with our mean-field theory, i.e., $\mathcal{P}\Delta\hat{H}\hat{\rho} = 0$ reduces to $\mathcal{P}\hat{\rho} = \otimes_i \hat{\rho}^{(i)}$. Here, $\hat{\rho}^{(i)}$ denotes the reduced density matrix defined by the partial trace $\hat{\rho}^{(i)} = \text{Tr}_i \{ \hat{\rho} \}$, which performs the trace over all atomic states except of the i^{th} atom. Next, it is useful to express the operator $\hat{P}_{ee}^{(i)} = \hat{A}_{-\omega_0}^{(i)} + \hat{A}_0^{(i)} + \hat{A}_{\omega_0}^{(i)}$ in terms of the projections onto the eigenstates of $\hat{H}_{\text{MF}}^{(i)}$, where $\hbar\omega_0 = 2h$ denotes the energy splitting of the mean-field Hamiltonian. Introducing the interaction picture with respect to $\sum_i \hat{H}_{\text{MF}}^{(i)}$ the interaction Hamiltonian $\hat{H}_{\text{int}}^{(i,j)}(t)$ within the rotating wave approximation reduces to

$$\hat{H}_{\text{int}}^{(i,j)}(t) = \sum_{\omega=0, \pm\omega_0} \frac{C_6}{|\mathbf{r}_i - \mathbf{r}_j|^6} \hat{A}_{\omega}^{(i)} \otimes \hat{A}_{\omega}^{(j)\dagger}. \quad (6)$$

The terms $\hat{A}_{\pm\omega_0}$ describe the exchanges of an excitation between the system $\hat{\rho}^{(i)}$ and the surrounding bath and is relevant for the equilibration of the time evolution, while the terms with \hat{A}_0 account for a dephasing. The second order time-convolutionless master equation [22, 23] for the reduced density matrix $\hat{\rho}^{(i)}(t)$ takes the form

$$\frac{d}{dt} \hat{\rho}^{(i)} = \sum_{\omega, \omega'} \gamma_{\omega\omega'} \left(\hat{A}_{\omega}^{(i)} \hat{\rho}^{(i)} \hat{A}_{\omega'}^{(i)\dagger} - \frac{1}{2} \left\{ \hat{A}_{\omega'}^{(i)\dagger} \hat{A}_{\omega}^{(i)}, \hat{\rho}^{(i)} \right\} \right),$$

with the rates

$$\gamma_{\omega\omega'} = \frac{512\pi^4 n t}{27\hbar^2} \frac{1}{a_R^9} \langle \hat{A}_{\omega'}^{(i)} \hat{A}_{\omega}^{(i)\dagger} \rangle. \quad (7)$$

Here, we have again used the translation invariance of the system in the critical region $\alpha \ll 1$ allowing us to replace the average over the j^{th} atom, with the local density matrix $\hat{\rho}^{(i)}(t)$. The master equation is a highly nonlinear equation for the local density $\hat{\rho}^{(i)}(t)$, where at each time step the mean-field $f_R = \text{Tr} \{ \hat{\rho}^{(i)} \hat{P}_{ee}^{(i)} \}$ and the rates $\gamma_{\omega, \omega'}$ have to be determined. We would like to stress that the master equation conserves energy with the above mean-field solution as a stationary state. The master equation can be efficiently solved numerically after a transformation back into the Schrödinger picture. In Fig. 2 the solution of the master equation (solid line) is compared to

the full dynamics (crosses). The pair-correlation function strongly influences the decoherence rates $\gamma_{\omega, \omega'}$. As the pair correlation is not determined self-consistently within our approach, we apply once a single fit for the effective Rabi frequency and the saturated Rydberg fraction to account for these corrections. Then, we find perfect agreement between the full dynamics and the solution of the master equation, see Fig. 2; the deviations at large times are accounted to the finite size effects of the full dynamics. The characteristic time scale of the oscillations is determined by the collective Rabi frequency $\sqrt{N_{\text{block}}}\Omega$, with $N_{\text{block}} \sim n a_R^3$ the number of atoms within the blocked volume of the van der Waals interaction.

In conclusion, we have established a universal scaling behavior in strongly interacting Rydberg gases due to the existence of a second order quantum phase transitions. It remains an open question, whether it is experimentally possible to reach the crystalline phase.

We acknowledge discussions with F. Robicheaux. The work was supported by the Deutsche Forschungsgemeinschaft (DFG) within SFB/TRR 21 and by Pf381/4-1.

* Electronic address: hweimer@itp3.uni-stuttgart.de

- [1] M. E. Fisher, Rev. Mod. Phys. **70**, 653 (1998).
- [2] W. R. Anderson, J. R. Veale, and T. F. Gallagher, Phys. Rev. Lett. **80**, 249 (1998).
- [3] K. Singer et al., Phys. Rev. Lett. **93**, 163001 (2004).
- [4] D. Tong et al., Phys. Rev. Lett. **93**, 063001 (2004).
- [5] T. Vogt et al., Phys. Rev. Lett. **97**, 083003 (2006).
- [6] R. Heidemann et al., Phys. Rev. Lett. **99**, 163601 (2007).
- [7] U. Raitzsch et al., Phys. Rev. Lett. **100**, 013002 (2008).
- [8] R. Heidemann et al., Phys. Rev. Lett. **100**, 033601 (2008).
- [9] T. A. Johnson et al., Phys. Rev. Lett. **100**, 113003 (2008).
- [10] T. Cubel et al., Phys. Rev. A **72**, 023405 (2005).
- [11] A. K. Mohapatra, T. R. Jackson, and C. S. Adams, Phys. Rev. Lett. **98**, 113003 (2007).
- [12] M. Reetz-Lamour et al., New J. Phys. **10**, 045026 (2008).
- [13] F. Robicheaux and J. V. Hernández, Phys. Rev. A **72**, 063403 (2005).
- [14] J. Stanojevic and R. Côté, arXiv:0801.2406 (2008).
- [15] C. Ates et al., Phys. Rev. A **76**, 013413 (2007).
- [16] J. Stanojevic and R. Côté, arXiv:0801.2396 (2008).
- [17] T. F. Gallagher, *Rydberg Atoms* (Cambridge University Press, Cambridge, 1994).
- [18] K. Singer et al., J. Phys. B **38**, S295 (2005).
- [19] F. Robicheaux, J. Phys. B **38**, S333 (2005).
- [20] T. Amthor et al., Phys. Rev. Lett. **98**, 023004 (2007).
- [21] J. V. Hernández and F. Robicheaux, J. Phys. B **41**, 045301 (2008).
- [22] H.-P. Breuer, Phys. Rev. A **75**, 022103 (2007).
- [23] H.-P. Breuer and F. Petruccione, *The Theory of Open Quantum Systems* (Oxford University Press, Oxford, 2002).